Bioresource Technology 282 (2019) 125–132

Contents lists available at ScienceDirect

Bioresource Technology

journal homepage: www.elsevier.com/locate/biortech

Silicate mediated simultaneous in-situ CO_2 sequestration and nutrients removal in anaerobic digestion

He Liu[a,b,c], Linlin Gong[a], Yan Zhang[a,b,c,*], Qianqian Jiang[a], Minhua Cui[a,b,c], Jie Zhang[a], Bo Fu[a,b,c], Hongbo Liu[a,b,c]

[a] *School of Environment and Civil Engineering, Jiangnan University, Wuxi 214122, China*
[b] *Jiangsu Key Laboratory of Anaerobic Biotechnology, Wuxi 214122, China*
[c] *Jiangsu Collaborative Innovation Center of Water Treatment Technology and Material, Suzhou 215011, China*

GRAPHICAL ABSTRACT

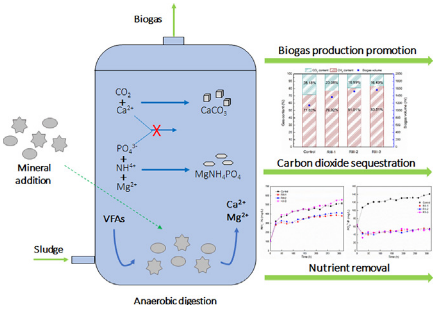

ARTICLE INFO

Keywords:
Anaerobic digestion
Mineral carbonation
CO_2 sequestration
Nutrients removal
Silicates

ABSTRACT

This study investigated the reactions among CO_3^{2-}, PO_4^{3-}, NH_4^+, Mg^{2+}, and Ca^{2+}, under different CO_3^{2-} concentration and Mg^{2+}/Ca^{2+} ratio, and conducted sludge anaerobic digestion (AD) with silicate addition to achieve in-situ CO_2 sequestration and nutrients removal. High CO_3^{2-} concentration facilitated the formation of $MgNH_4PO_4$, and Mg^{2+}/Ca^{2+} ratio of 1:1 achieved best CO_3^{2-}, PO_4^{3-}, and NH_4^+ removal in simulated anaerobic digestate. Supplementation of 40 g/L magnesium silicate combined with 20 g/L wollastonite decreased CO_2 content in biogas from 28.2% to 19.0%, and removed PO_4^{3-} and NH_4^+ by 61.8% and 21.2%, respectively, in AD. Simultaneous in-situ CO_2 sequestration and nutrients removal was achieved by directed precipitation of PO_4^{3-}, NH_4^+, and CO_2 with silicate released Mg^{2+} and Ca^{2+}, to form $MgNH_4PO_4$ and $CaCO_3$. Meanwhile, methane production was improved by 51.2% with silicate supplementation. This study provides an attractive measure for CO_2 and nutrients removal as well as methane production enhancement of sludge AD.

1. Introduction

Reduction of anthropogenic greenhouse gases (GHGs) emission is a crucial issue for climate change mitigation (Choi et al., 2009). Wastewater treatment plants (WWTPs) are recognized as one of the main secondary sources of GHGs emissions, which produce GHGs during the treatment processes (Shahabadi et al., 2010) as well as CO_2 emission from the energy consumption of the plants operation (Shahabadi et al., 2009). Controlling GHGs emissions during wastewater treatment and achieving carbon neutrality WWTPs operation is of great significance to

---

[*] Corresponding author at: School of Environment and Civil Engineering, Jiangnan University, Wuxi 214122, China.
E-mail address: yanzhang@jiangnan.edu.cn (Y. Zhang).

https://doi.org/10.1016/j.biortech.2019.03.004
Received 11 January 2019; Received in revised form 25 February 2019; Accepted 1 March 2019
Available online 01 March 2019

global GHGs reduction and climate change mitigation.

Anaerobic digestion (AD) is the most widely used technology in the field of sludge treatment in developed countries, for its sludge stabilization, especially energy recovery ability, which benefits to achieve carbon neutrality in WWTPs (Gu et al., 2017; Jenicek et al., 2012). However, the produced biogas can not be directly utilized, owing to the high CO_2 content of 30–50 vol% and relatively low methane content of 50–70% (Angelidaki et al., 2018). Commercially available technologies for biogas upgrading have increased biogas production costs by 20–72% due to energy, chemicals and water consumption, and may result in up to 8% methane losses (Sun et al., 2015). In addition, CO_2 is usually released into the atmosphere during the regeneration of the adsorbent in the biogas upgrading process (Lombardi and Carnevale, 2013), which aggravates global warming. Developing CO_2 in situ sequestration in AD is a feasible solution to improve the economics of AD process, and reduce carbon emission during sludge treatment (Fernandez et al., 2017).

Mineral CO_2 sequestration is a process that CO_2 is fixed in the form of carbonates by reacting with alkaline silicates, mainly calcium and magnesium silicates such as wollastonite ($CaSiO_3$), olivine (mainly Mg_2SiO_4), forsterite ($Mg_{1.82}Fe_{0.18}SiO_4$), serpentine ($Mg_3Si_2O_5(OH)_4$) (Azdarpour et al., 2015; Bearat et al., 2006; Farhang et al., 2016). The slow release of alkalinity and divalent cations from alkaline silicate minerals limits CO_2 sequestration rate at ambient environmental conditions. However, mineral CO_2 sequestration can be integrated in two-stage biotechnological processes that involve a sequence of an acid- and an alkalinity-producing step (Salek et al., 2013). AD is essentially a two-stage process with firstly volatile fatty acids (VFAs) production from complex organic matters, and subsequently methane production using VFAs as the substrate, which can be well coupled with mineral CO_2 sequestration. The former stage, VFAs fermentation, can provide the necessary acidity to dissolve silica minerals and release cations, while the latter stage, methanogenesis, provides alkalinity for carbonates formation. With wollastonite or olivine addition in sludge AD, mineral carbonation has been preliminarily achieved (Linville et al., 2016b; Zhang et al., 2018b). Mineral CO_2 sequestration has been considered as a promising in-situ CO_2 capture and biogas upgrading technology for sludge AD.

However, a large amount of NH_4^+-N and PO_4^{3-}-P, up to 1000 mg/L, can be released during sludge AD (Praveen et al., 2018; Wang et al., 2015), due to the degradation of organic matters. The high concentration of NH_4^+ and PO_4^{3-} may attenuate CO_2 carbonation by competing cations. It is known that phosphate severely inhibits the formation of carbonate precipitates (Cao and Harris, 2008). Previous study has also found that PO_4^{3-} consumed mineral released Ca^{2+} and formed calcium phosphate ($Ca_3(PO_4)_2$) in wollastonite added sludge AD (Zhang et al., 2018b). Magnesium phosphate is hard to generate in AD environment, however, magnesium ammonium phosphate (MAP) may form in magnesium silicate added sludge AD, though it was not mentioned in the previous reports (Linville et al., 2016a, b). As formation of $Ca_3(PO_4)_2$ and/or $MgNH_4PO_4$ consumes cation released from silicate and reduces carbonate precipitate amount, the interference of NH_4^+ and PO_4^{3-} is supposed to be prevented for higher CO_2 sequestration performance. However, the solubility product constant (K_{sp}) at 25 °C of $Ca_3(PO_4)_2$ and $MgNH_4PO_4$ is 2.073×10^{-33} and 3×10^{-13}, respectively, much lower than that of $CaCO_3$ (3.36×10^{-9}), which indicates that it is almost impossible to prevent the formation of $Ca_3(PO_4)_2$ and/or $MgNH_4PO_4$ in alkalinity silicate added sludge AD. Nevertheless, it provides an opportunity for simultaneous in-situ CO_2 sequestration and nutrients removal in sludge AD.

The influence of nutrients on mineral CO_2 sequestration has been noticed (Zhang et al., 2018b), however, simultaneous nutrients removal coupled with mineral CO_2 sequestration has not been proposed. The purpose of this study is to investigate and achieve the best performance of simultaneous in-situ CO_2 sequestration and nutrients removal in sludge AD with silicate supplementation. Currently, single type of silicate mineral, i.e. calcium silicate like wollastonite, or magnesium silicate like olivine, was used for mineral CO_2 sequestration in sludge AD (Lindeboom et al., 2013; Linville et al., 2016a, b; Zhang et al., 2018b). If applying calcium silicate, only PO_4^{3-} can be removed by forming $Ca_3(PO_4)_2$. Whereas using magnesium silicate, both NH_4^+ and PO_4^{3-} may be reduced if MAP forms. However, the CO_2 sequestration potential of magnesium silicate is lower than calcium silicate, owing to higher solubility and lower stability of $MgCO_3$ ($k_{sp} = 6.82 \times 10^{-6}$ at 25 °C) than $CaCO_3$ ($k_{sp} = 3.36 \times 10^{-9}$ at 25 °C). Therefore, combined application of calcium and magnesium silicates was adopted in this study. Firstly, the effect of CO_3^{2-} concentration on the reactions among Mg^{2+}, Ca^{2+}, NH_4^+, and PO_4^{3-} was analyzed, to reveal that if the variation of alkalinity during AD process would affect on the simultaneous removal of NH_4^+ and PO_4^{3-} by precipitation. Subsequently, the effect of Mg^{2+}/Ca^{2+} ratio on CO_3^{2-}, NH_4^+, and PO_4^{3-} removal by precipitation was analyzed in simulated anaerobic digestate liquid. Finally, magnesium and calcium silicates mediated simultaneous in-situ CO_2 sequestration and nutrients removal was achieved in the AD system with the optimum Mg^{2+}/Ca^{2+} ratio obtained in the precipitation experiment. The mechanism and the strategy for further application of magnesium and calcium silicates mediated simultaneous in-situ CO_2 sequestration and nutrients removal in sludge AD was also discussed.

2. Materials and methods

2.1. Substrate, inoculum, and silicates

Sludge hydrolysate was used as the substrate of AD in this study. The sludge was taken from the dewatered sludge tank of a local wastewater treatment plant (WWTP) in Wuxi City. The sludge had total solids (TS) of 136.0 ± 1.0 g/L and volatile solids/total solids (VS/TS) of 53.7 ± 0.9%. The sludge was diluted to TS of 60 g/L, and treated under 100 °C for 24 h. After thermal treatment, the sludge was centrifuged under 8000 rpm for 10 min. The supernatant after centrifugation was the sludge hydrolysate used as the substrate. The properties of the substrate are shown in Table 1. The inoculum was anaerobic granular sludge taken from an up-flow anaerobic sludge bed (UASB) reactor of another local WWTP. The properties of the anaerobic granular sludge were TS 6.1 ± 0.1%, VS/TS 58.8 ± 0.2%, pH 7.2 ± 0.2. The wollastonite same with previous reported (Zhang et al., 2018b), was used as calcium silicate in this study. The wollastonite was screened with 120 mesh, and had the average particle size of 21.0 μm. The magnesium silicate used in this study was AR grade purchased from Sinopharm Chemical Reagent Co., Ltd.

2.2. Precipitation under different CO_3^{2-} concentration

Four water solutions with PO_4^{3-} of 6 mM and NH_4^+ of 50 mM were prepared to simulate the nutrient concentration in anaerobic digestate liquid. The CO_3^{2-} concentration in the four water solutions were set as 0 mM, 3 mM, 6 mM, and 12 mM, respectively, for investigating the effect of CO_3^{2-} concentration on the reactions among Mg^{2+}, Ca^{2+},

Table 1
Characteristics of the sludge hydrolysate.

pH	COD (mg/L)	NH_4^+-N (mg/L)	PO_4^{3-}-P (mg/L)	Soluble Protein (mg/L)	Soluble Polysaccharide (mg/L)
7.5 ± 0.1	12025 ± 21	107.9 ± 2.6	63.1 ± 2.4	232.2 ± 4.8	1269.0 ± 0.8

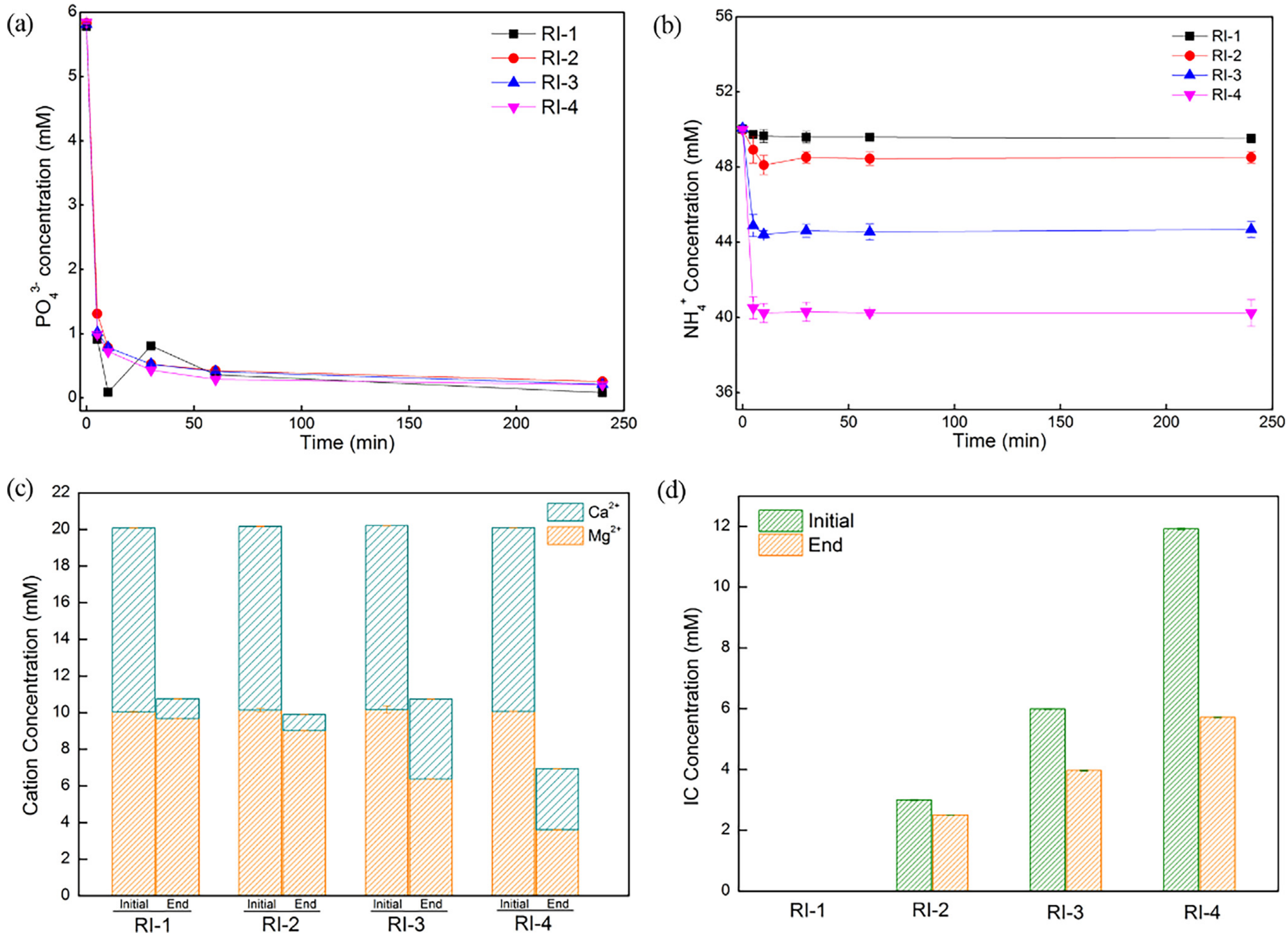

Fig. 1. Variation of ion concentration during reaction under different initial CO_3^{2-} concentration. (a) PO_4^{3-} concentration; (b) NH_4^+ concentration; (c) Mg^{2+}, Ca^{2+} concentration; (d) IC concentration.

NH_4^+, and PO_4^{3-}. The pH of the four water solutions were adjusted to 7.5 before reaction. The reactions were carried out in 500 ml glass bottles with 250 ml solution. The bottles were purged with N_2 gas at a rate of 0.5 L/min for 20 min to eliminate the CO_2 in the headspace. Equal Mg^{2+} and Ca^{2+} of 10 mM were rapidly added into the liquid to start precipitation reactions. The reactions under CO_3^{2-} concentration of 0 mM, 3 mM, 6 mM, and 12 mM were named as RI-1, RI-2, RI-3, and RI-4, respectively. All the reactions were conducted under temperature of 35.0 ± 0.5 °C and stirring of 120 rpm in triplicates. Na_2HPO_4, NH_4Cl, Na_2CO_3, $MgCl_2$, and $CaCl_2$ were used to provide PO_4^{3-}, NH_4^+, CO_3^{2-}, Mg^{2+}, and Ca^{2+}, respectively. Samples were periodically taken during reaction to measure the pH, CO_3^{2-}, NH_4^+, PO_4^{3-}, Mg^{2+}, and Ca^{2+}. The precipitates were collected at the end of reactions, and analyzed by scanning electron microscopy (SEM) and X-ray diffraction (XRD).

2.3. *Precipitation under different Mg^{2+}/Ca^{2+} ratio*

Water solution with PO_4^{3-} 6 mM, NH_4^+ 50 mM, CO_3^{2-} 12 mM, and pH 7.5 was prepared to simulate the anaerobic digestate liquid. The reactions were carried out in 500 ml glass bottles with 250 ml simulated digestate liquid. The bottles were purged with N_2 gas at a rate of 0.5 L/min for 20 min to eliminate the CO_2 in the headspace. Total 20 mM cations (Mg^{2+} and/or Ca^{2+}) were rapidly added into the liquid to start precipitation reactions. For investigating the ratio of Mg^{2+}/Ca^{2+} on final composition of the precipitates, reactions under five Mg^{2+}/Ca^{2+} ratio, i.e. 20 mM:0 mM, 14 mM:6 mM, 10 mM:10 mM, 6 mM:14 mM, 0 mM:20 mM, was conducted, named as RII-1, RII-2, RII-3, RII-4, and RII-5, respectively. All the reactions were conducted under temperature of 35.0 ± 0.5 °C and stirring of 120 rpm in triplicates.

2.4. *Operation of the AD processes*

The AD processes was carried out in 800 ml glass reactors with an effective volume of 400 ml. 320 ml sludge hydrolysate and 80 ml seed sludge was mixed and fed into the digesters. The initial pH in the digesters was adjusted to 7.5. Three digesters were operated with silicate addition. The first one was added with 32 g magnesium silicate (dosage of 80 g/L), and named as RIII-1. The second one was added with 16 g magnesium silicate (40 g/L) and 8 g wollastonite (20 g/L), named as RIII-2. The last one was added with 16 g wollastonite (40 g/L), and named as RIII-3. The added silicates were filled in 3500 D dialysis bags. 16 g magnesium silicate and 8 g wollastonite could provide similar amount of Mg^{2+} and Ca^{2+} in weak acid environment (data shown in E-supplementary data). The digester without silicate addition was operated as the control. The reactors was purged with N_2 gas for 20 min at a rate of 0.5 L/min to ensure an anaerobic environment before digestion. A gas bag was installed on the top of each digester for biogas collection. The AD experiments were operated in batch mode under temperature of 35 °C. Liquid samples were taken and analyzed periodically during anaerobic digestion. Gas samples were analyzed at the end of digestion.

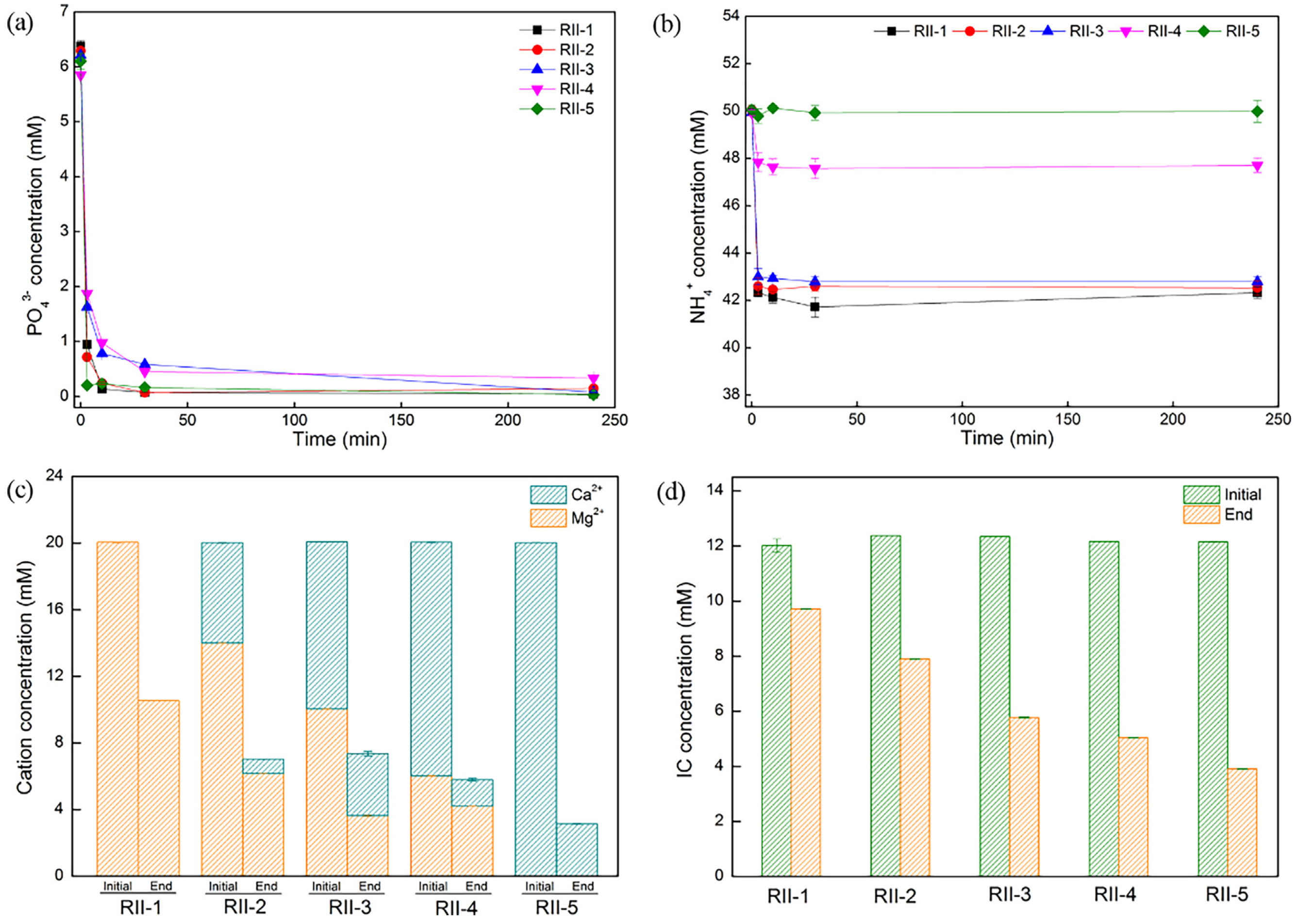

Fig. 2. Variation of ion concentration during reaction under different initial Mg^{2+}/Ca^{2+} ratio. (a) PO_4^{3-} concentration; (b) NH_4^+ concentration; (c) Mg^{2+}, Ca^{2+} concentration; (d) IC concentration.

2.5. Analysis methods

COD, PO_4^{3-}-P, NH_4^+-N, and pH were determined according to standard methods (China, 2002). Inorganic carbon (IC) was measured using a TOC detector (TOC-V_{CPH}, Shimadzu, Japan). Mg^{2+} and Ca^{2+} concentrations were determined by atomic absorption spectrophotometer (AA 7700, Shimadzu, Japan). Gas component was analyzed by a gas chromatography (GC9790II, FULI, China) with a thermal conductivity detector (TCD) and a stainless steel packed column (AE. TDX-01, 2 m × 3 mm). The volume of the produced biogas was measured by displacement of saturated aqueous NaCl in a graduated measuring cylinder (Abouelenien et al., 2009). The gas volume was calibrated to standard conditions (273 K, 1 atm) after measurement. The SEM and XRD analysis were conducted using a SU1510 (Hitachi, Japan) and a D8 Advance DMAX2RB (Bruker, Germany).

3. Results and discussion

3.1. Effect of CO_3^{2-} concentration on the reactions among Mg^{2+}, Ca^{2+}, NH_4^+, and PO_4^{3-}

The variation of ion concentration during the precipitation reactions among Mg^{2+}, Ca^{2+}, CO_3^{2-}, NH_4^+, and PO_4^{3-} are shown in Fig. 1. The PO_4^{3-} concentration decreased rapidly by 4.5–4.9 mM in the first 5 min, account for 77.6–84.0% of initial PO_4^{3-} amount. The final removal of PO_4^{3-} reached 95.7–98.6% in all the reactions, indicated that CO_3^{2-} concentration did not significantly impact on PO_4^{3-} removal. However, the removal of NH_4^+ increased significantly along with CO_3^{2-} concentration increase. The decrease of NH_4^+ concentration was 0.4 mM, 1.6 mM, 5.4 mM, and 9.6 mM, under initial CO_3^{2-} concentration of 0 mM, 3 mM, 6 mM, and 12 mM, respectively. The decrease of cation concentration was also influenced by the CO_3^{2-} concentration (Fig. 1c). The Ca^{2+} was decreased by 9.0 mM and 9.1 mM in RI-1 and RI-2, i.e. initial CO_3^{2-} concentration of 0 mM and 3 mM, respectively. While the decrease of Mg^{2+} was only 0.3 mM and 1.0 mM in RI-1 and RI-2, respectively. As no CO_3^{2-} added in R1-1 and almost no change in NH_4^+ and Mg^{2+} concentration (Fig. 1d), the decrease of Ca^{2+} and PO_4^{3-} could be attributed to the precipitation between Ca^{2+} and PO_4^{3-}. With slight change of NH_4^+, Mg^{2+}, and CO_3^{2-} in RI-2, the precipitation by Ca^{2+} and PO_4^{3-} was still the dominant reaction. With increase of initial CO_3^{2-} concentration, the removal of NH_4^+ and Mg^{2+-} increased in RI-3 and RI-4, which indicated that MAP might generate in these two reactions.

The XRD pattern of the precipitates formed in RI-2 with low CO_3^{2-} concentration of 3 mM and in RI-4 with high CO_3^{2-} concentration of 12 mM are shown in E-supplementary data. Low crystallinity of the precipitates formed in RI-2 was indicated by the diffuse peak shape. The XRD pattern was generally consistent with the standard pattern of Tricalcium Bis (phosphate(V)) ($Ca_3(PO_4)_2$, PDF#70-0364), confirmed the precipitation between Ca^{2+} and PO_4^{3-} in RI-2. The XRD pattern of the precipitates from RI-4 was generally consistent with the combined standard pattern of struvite ($NH_4MgPO_4{\cdot}6H_2O$, PDF#15–0762) and calcite ($CaCO_3$, PDF#51–1524), which confirmed the formation of MAP. It revealed that under low CO_3^{2-} concentration, the formation of $Ca_3(PO_4)_2$ overcame that of MAP and $CaCO_3$, resulted in the simultaneous decrease of Ca^{2+} and PO_4^{3-}, but almost no change in NH_4^+

concentration. While high CO_3^{2-} concentration promoted the formation of MAP, thus the Ca^{2+} precipitated with CO_3^{2-} by formation of $CaCO_3$. Therefore, under the high CO_3^{2-} concentration, the Mg^{2+} and Ca^{2+} were directional allocated to generate MAP and $CaCO_3$, respectively, which achieved best simultaneous removal of PO_4^{3-}, NH_4^+, and CO_3^{2-} in RI-4. Considering the alkalinity (mainly CO_3^{2-}) in digesters increase during AD process, and normally excess 1200 mg/L (12 mM) at the end of digestion (Fonoll et al., 2015), directed precipitation of Mg^{2+} and Ca^{2+} to MAP and $CaCO_3$ could be achieved in AD, and realize simultaneous removal of PO_4^{3-} and NH_4^+, and CO_2 sequestration.

3.2. *Effect of Mg^{2+}/Ca^{2+} ratio on precipitation products of Mg^{2+}, Ca^{2+}, CO_3^{2-}, NH_4^+ and PO_4^{3-}*

The variation of ion concentration after cation addition are shown in Fig. 2. The concentration of PO_4^{3-} decreased immediately after cation added, and was removed by 5.5–6.3 mM, accounted for 94.4–99.4% of initial PO_4^{3-} in the five groups, after 240 min reaction. The removal of PO_4^{3-} was not affected by the ratio of Mg^{2+}/Ca^{2+}, as PO_4^{3-} can precipitate with both Ca^{2+} and Mg^{2+}. The removed amount of NH_4^+ in RII-1, RII-2, RII-3, RII-4, and RII-5 were 7.8 mM, 7.4 mM, 7.2 mM, 2.3 mM, and 0.2 mM, respectively, which indicated that the removal of NH_4^+ was greatly affected by the ratio of Mg^{2+}/Ca^{2+}. The NH_4^+ could effectively removed in RII-1, RII-2, and RII-3, in which the ratio of Mg^{2+}/Ca^{2+} was 20 mM:0 mM, 14 mM:6 mM, and 10 mM:10 mM, respectively. It is conceivable that the poor removal of NH_4^+ in RII-5, as the NH_4^+ can not precipitate with the single cation, Ca^{2+}. However, the NH_4^+ removal in the RII-4 was also relatively low, where initial Mg^{2+} was 6 mM and sufficient for removing both NH_4^+ and PO_4^{3-} by 6 mM if the Mg^{2+} formed MAP. The low NH_4^+ removal in RII-4 indicated that few MAP was formed, which was consistent with the low decrease of Mg^{2+} (Fig. 2c). The removal of CO_3^{2-} was 2.4 mM, 4.5 mM, 6.6 mM, 7.1 mM, and 8.2 mM in RII-1, RII-2, RII-3, RII-4, and RII-5, respectively, which indicated that the removal of CO_3^{2-} was negatively correlated with the ratio of Mg^{2+}/Ca^{2+}. The removal of CO_3^{2-} was higher in high Ca^{2+} concentration groups than the high Mg^{2+} concentration ones, confirmed the higher CO_2 sequestration potential of calcium silicate than magnesium silicate (Zhang et al., 2018b). As PO_4^{3-} removal was not significantly affected by the ratio of Mg^{2+}/Ca^{2+}, NH_4^+ removal and CO_3^{2-} removal were the two key parameters to determine the optimum ratio of Mg^{2+}/Ca^{2+} for simultaneously PO_4^{3-}, NH_4^+, and CO_3^{2-} removal. Though, the removal of CO_3^{2-} in RII-4 and RII-5 was slightly higher than that in RII-3, the removal of NH_4^+ in RII-4 and RII-5 was significantly lower than that in RII-3. In addition, RII-3 achieved the similar NH_4^+ removal and higher CO_3^{2-} removal compared to that in RII-4 and RII-5. Therefore, the Mg^{2+}/Ca^{2+} ratio of 10 mM: 10 mM adopted in RII-3 was the optimum ratio for simultaneous CO_2 sequestration and nutrients removal.

The precipitates formed in the reactions were collected and analyzed by XRD. The XRD patterns of the precipitates are shown in E-supplementary data. The XRD pattern of the precipitate formed in RII-1 was consistent with the standard pattern of struvite (PDF#71-2089), indicated that MAP was the main component of the precipitate in the reaction with 20 mM Mg^{2+} addition only. It was consistent with the similar removed molar amount of PO_4^{3-} and NH_4^+ (Fig. 2). In the reaction with 20 mM Ca^{2+} addition only, i.e. RII-5, the precipitate was identified as $CaCO_3$ and $CaHPO_4$, as its XRD pattern was consistent with the combined standard pattern of calcite (PDF#05-0586) and brushite (PDF#72-1240). The high removal of PO_4^{3-} and CO_3^{2-}, and the no removal of NH_4^+ was well consistent with the formation of $CaCO_3$ and $CaHPO_4$. In the reactions with both Mg^{2+} and Ca^{2+} added, the components of the precipitates were also not the same. In RII-4, where the ratio of Mg^{2+}/Ca^{2+} was 6 mM:14 mM, the XRD pattern precipitate was similar with that of R5, consistent with the combined standard pattern of calcite and brushite. In RII-2 and RII-3, where the ratio of Mg^{2+}/Ca^{2+} was 14 mM:6 mM and 10 mM: 10 mM, the precipitates were identified as struvite and calcite. It indicated that the NH_4^+ was removed in the only form of MAP. As PO_4^{3-} and NH_4^+ is removed equally, in stoichiometry, by forming MAP, and the concentration of PO_4^{3-} was lower than that of NH_4^+ in anaerobic digestate, the removal of NH_4^+ was limited to the amount of PO_4^{3-} in the liquid. Less MAP formed in reactions with Mg^{2+}/Ca^{2+} ratio lower than 10 mM:10 mM, was owing to that relatively high concentration of Mg^{2+} promotes the formation of MAP, while low Mg^{2+}/Ca^{2+} ratio benefits the formation of Ca-P precipitates (Cao and Harris, 2008; Harris et al., 2008). With increase of Mg^{2+}/Ca^{2+} ratio, PO_4^{3-} was precipitated in form of MAP instead of Ca-P precipitate. In this case, NH_4^+ and PO_4^{3-} could simultaneously precipitated with Mg^{2+}. In the RII-3, with equal Mg^{2+} and Ca^{2+} of 10 mM, the best performance of simultaneous CO_3^{2-} and nutrients removal was achieved by directed precipitation of Mg^{2+} and Ca^{2+} to form MAP and $CaCO_3$, respectively. Therefore, Mg^{2+}/Ca^{2+} ratio of 10 mM:10 mM, i.e. equimolar of Mg^{2+} and Ca^{2+}, was expected to achieve simultaneous NH_4^+ and PO_4^{3-} removal, and CO_2 sequestration in AD.

3.3. *Performance of CO_2 sequestration and nutrients removal in AD with silicate addition*

Magnesium silicate and calcium silicate (wollastonite) were adopted to achieve CO_2 sequestration and nutrients removal in AD. For best simultaneous NH_4^+ and PO_4^{3-} removal, and CO_2 sequestration, the amount of Mg^{2+} and Ca^{2+} released from silicate should be closed to 1:1, according to the precipitation experiments. The digester RIII-2 was added with 16 g magnesium silicate and 8 g wollastonite, which was expected to release similar amount of Mg^{2+} and Ca^{2+} according to cation release experiment (E-supplementary data). The dissolution of magnesium silicate was slower than that of calcium silicate as reported (Kerisit et al., 2013; Lindeboom et al., 2013). Therefore, more magnesium silicate was added to obtain the same amount of cation. RIII-1 with 32 g magnesium silicate addition and RIII-3 with 16 g wollastonite addition were operated to confirm if the RIII-2 would achieve the best NH_4^+ and PO_4^{3-} removal, and CO_2 sequestration performance.

3.3.1. *Biogas production in silicate added AD*

The biogas production and the gas content of the ADs with silicate addition are shown in Fig. 3. The biogas production of the RIII-1, RIII-2, and RIII-3 were 1363 ml, 1524 ml, and 1560 ml, respectively, higher than that of control (1136 ml). The methane production of RIII-1, RIII-2, and RIII-3 were 1048 ml, 1234 ml, and 1303 ml, respectively, also higher than that of control (816 ml). It indicated the improvement of methane production in AD with silicate addition. Consistent with the improved biogas production, the COD degradation in silicate added reactors was higher than that of control (Fig. 4a). One of the possible

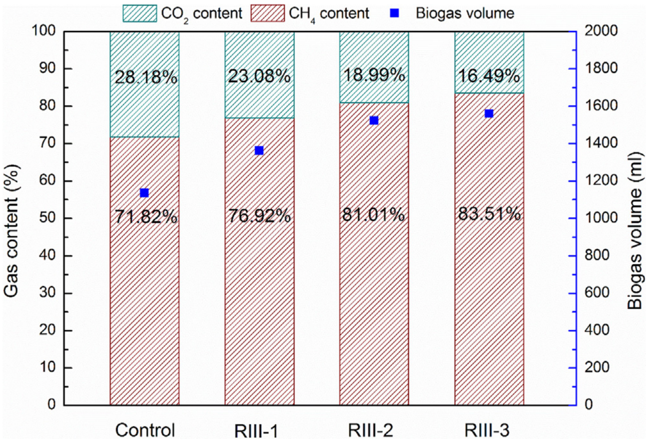

Fig. 3. Biogas production characteristics of the ADs with silicate addition.

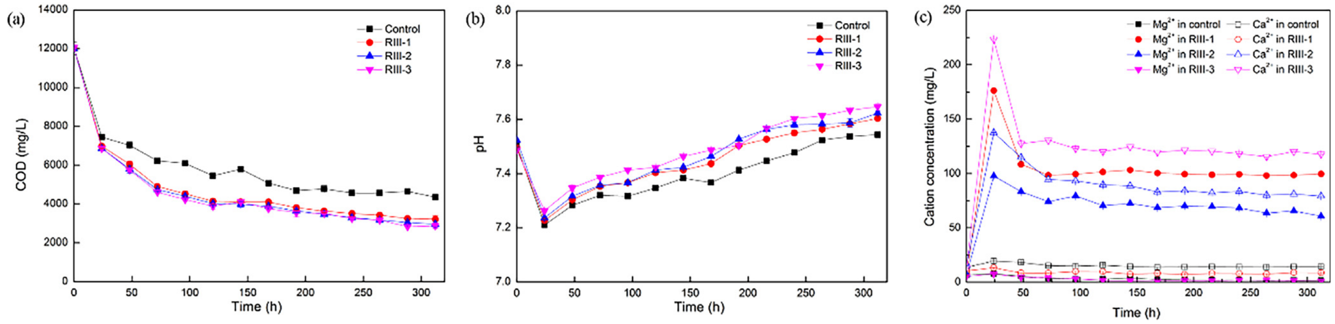

Fig. 4. (a) COD, (b) pH, (c) Mg^{2+} and Ca^{2+} profiles during the ADs with silicate addition.

reasons for methane production enhancement by silicate addition is pH buffering (Linville et al., 2016b; Zhang et al., 2018b). With VFAs production from complex organic compounds, pH usually decreases in the early stage of AD, which may inhibit methanogenic activity (Montanes et al., 2014; Zhang et al., 2018a). With silicate addition, the pH could buffered by proton consumption during cation release (Lindeboom et al., 2013). The pH in silicate added RIII-1, RIII-2, and RIII-3 was indeed higher than that of control (Fig. 4b). Considering the lowest pH in the control was 7.21, which was not very low for inhibiting methanogenesis, methane production enhancement based on de-inhibition was limited. However, the increased alkaline pH with silicate addition could also improve methane production based on facilitating hydrolysis of organic matter. Another possible reason for methane production enhancement is the increased Ca^{2+}/Mg^{2+} concentration. Moderate addition of Ca^{2+} or Mg^{2+} (less than 1000 mg/L) could improve biogas production of AD up to 30% (Dang et al., 2014; Kumar et al., 2016), though higher concentration of Ca^{2+} or Mg^{2+} showed negative impact (Dang et al., 2014; Kumar et al., 2016; Yin et al., 2018). With silicate addition, the Mg^{2+} and/or Ca^{2+} in RIII-1, RIII-2, and RIII-3 was higher than that in the control (Fig. 4c), due to the release of Mg^{2+} and/or Ca^{2+} from silicates. The release of Mg^{2+} and Ca^{2+} from the silicates was dramatically in the first 24 h, consistent with the pH decrease in this stage. Afterwards, the Mg^{2+} and Ca^{2+} concentration declined rapidly, and kept relatively stable after 72 h. The enhancement of methane production in RIII-1, RIII-2, and RIII-3 was 28.4%, 51.2%, and 59.7%, compared to that of control. The result indicated the higher methane production enhancement potential of wollastonite than magnesium silicate, which was supported by the higher methane production improvement in the wollastonite added sludge AD (Zhang et al., 2018b) than the olivine added sludge AD (Linville et al., 2016b).

3.3.2. CO_2 sequestration in silicate mediated AD

The CO_2 content in RIII-1, RIII-2, and RIII-3 was 23.1%, 19.0%, and 16.5%, respectively, higher than that in the control (28.2%), indicated the achievement of CO_2 sequestration based on mineral carbonation in silicate added ADs. By assuming biogas content in silicate added ADs were consistent with that in the control before CO_2 carbonation, the sequestrated CO_2 in RIII-1, RIII-2, and RIII-3 was estimated as 69.5 ml, 140.1 ml, and 182.5 ml, and account for 18.1%, 32.6%, and 41.5% of the generated CO_2, respectively. With olivine supplementation of 25–50 g/L, the reduced CO_2 content in sludge AD was 1.2–3.7% (Linville et al., 2016b). With wollastonite addition of 16.25 g/L, the reduced CO_2 content in sludge AD was 1.4–6.1% (Zhang et al., 2018b). The reduced CO_2 content in this study (5.1–11.7%) was much higher than these two reports, probably owing to higher dosage adopted, i.e. 80 g/L magnesium silicate in RIII-1, 40 g/L magnesium silicate and 20 g/L wollastonite in RIII-2, and 40 g/L wollastonite in RIII-3. The higher pH (7.60–7.65) at the end of digestion in this study compared to that (7.14–7.47) in the wollastonite added sludge AD (Zhang et al., 2018b), might be another factor for the higher CO_2 sequestration performance, as alkaline pH facilitates carbonate precipitation. The reduced CO_2 content (1.4–6.1%) in low dosage (16.25 g/L) wollastonite added sludge AD (Zhang et al., 2018b) was higher than the reduced CO_2 content (1.2–3.7%) in high dosage (25–50 g/L) olivine added digesters (Linville et al., 2016b). Similarly, in this study, the RIII-3 with 16 g wollastonite addition achieved best CO_2 sequestration performance, much higher than that of RIII-1 with 32 g magnesium silicate addition, indicate the higher CO_2 sequestration potential of wollastonite than magnesium silicate. The decreased CO_2 content in RIII-2 with 16 g magnesium silicate and 6 g wollastonite addition was slightly lower than that in RIII-3, however, much higher than that in RIII-1, showed the good CO_2 sequestration performance with combined applying of magnesium silicate and wollastonite.

3.3.3. Decrease of PO_4^{3-} and NH_4^+ in AD with silicate addition

The variation of PO_4^{3-} and NH_4^+ concentration during digestion were shown in Fig. 5. The concentration of PO_4^{3-} and NH_4^+ increased in the control during the whole digestion process. With silicate addition, the PO_4^{3-}-P in RIII-1, RIII-2, and RIII-3 were 86.8 mg/L, 87.8 mg/L, and 89.7 mg/L lower than the control at the end of digestion, with

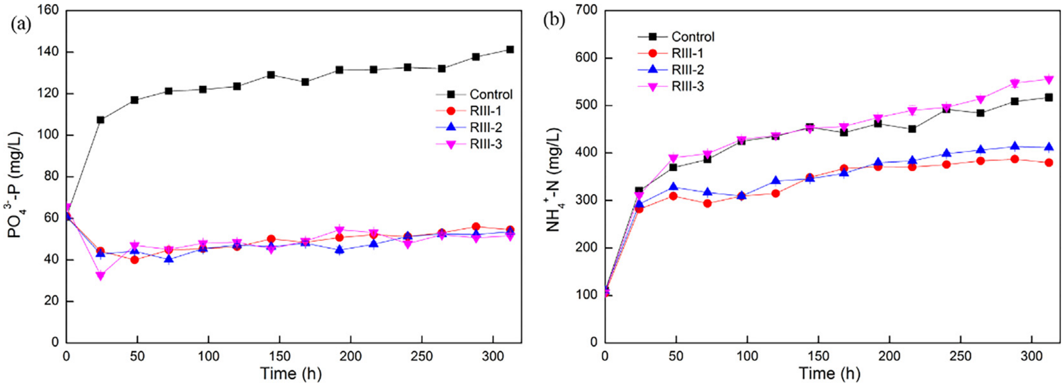

Fig. 5. (a) PO_4^{3-}-P, (b) NH_4^+-N concentration profiles during the ADs with silicate addition.

removal of 60.7%, 61.7%, and 62.5%, respectively. The final PO_4^{3-} concentration in RIII-1, RIII-2, and RIII-3 was similar, consistent with the results of precipitation experiment under different Mg^{2+}/Ca^{2+} ratio (Fig. 2a). The NH_4^+ concentration in RIII-3 was similar with the control during the digestion, indicated that NH_4^+ can not be removed by wollastonite addition. The higher NH_4^+ concentration in RIII-3 at the end of digestion could be attributed to the enhancement of organic matter degradation by wollastonite addition (Fig. 4a). The NH_4^+ concentration in RIII-1 and RIII-2, however, was 140 mg/L and 110 mg/L, account for 26.9% and 21.2%, lower than that of control.

The decreased PO_4^{3-} and NH_4^+ concentration as well as reduced CO_2 content were precipitated by reaction with Mg^{2+} and/or Ca^{2+} in the AD reactors. The Mg^{2+} and Ca^{2+} concentration decreased rapidly after 24 h digestion. The Mg^{2+} and Ca^{2+} concentration in RIII-2 at the end of digestion was 2.5 mM and 2.0 mM, respectively, close to the ratio of 1:1. The SEM photos of the precipitates formed in the reactors are shown in E-supplementary data. In RIII-1, the precipitates were mainly cuboid crystal with small amount of fine particles. In RIII-2, the cuboid crystal was still formed combined with some irregular shape particles. While in RIII-3, the precipitates were mainly irregular shape particles with some small cube crystal. The precipitates were identified as MAP and $MgCO_3$ in RIII-1, MAP and $CaCO_3$ in RIII-2, and $CaCO_3$ and monetite ($CaHPO_4$) in RIII-3, based on XRD pattern (E-supplementary data).

The composition of the precipitates in RIII-1, RIII-2, and RIII-3 were almost consistent with that in RII-1, RII-3, RII-5 of the precipitation experiments. It indicated that the precipitation between the ions was conducted as desired with silicate addition. The high concentration of IC at the end of digestion (434.9–479.1 mg/L) promoted the formation of MAP. Wollastonite addition captured CO_2 well in RIII-3, however, did not remove any NH_4^+; magnesium silicate addition removed NH_4^+ well in RIII-1, however, captured the least CO_2 among the three reactors. The best simultaneous in-situ CO_2 sequestration and nutrients removal was achieved in the AD with 16 g magnesium silicate and 8 g wollastonite addition, as predicted based on precipitation experiments.

According to the precipitation experiments, the ratio of Mg^{2+}/Ca^{2+} can influence the composition of the formed precipitates, thus impact on the removal of nutrients and CO_2. High Mg^{2+}/Ca^{2+} ratio attenuated CO_2 sequestration, while low Mg^{2+}/Ca^{2+} ratio significantly decreased NH_4^+ removal. The equimolar amount of Mg^{2+} and Ca^{2+} was the optimum ratio for simultaneous CO_2 sequestration and nutrients removal. For achieving the best simultaneous in-situ CO_2 sequestration and nutrients removal in sludge AD with silicate addition, the ratio of magnesium silicate and calcium silicate dosage should be determined based on their dissolve rate, to ensure that similar amount of Ca^{2+} and Mg^{2+} could be released in the sludge AD. The remained Mg^{2+} and Ca^{2+} (60.5–117.7 mg/L, Fig. 4c) in the silicate added reactors after digestion might be due to the chelation by chelating organic matters like humic acid. A higher dosage of the silicates may further enhance the performance of CO_2 sequestration and nutrients removal. As the NH_4^+ and PO_4^{3-} is removed in equimolar, in theory, by precipitation as MAP, the removal of NH_4^+ is relatively low owing to its higher concentration than that of PO_4^{3-} in sludge AD. However, high concentration of free ammonia may exist under high NH_4^+ level in sludge AD, which usually causes inhibition of methanogenesis (Chen et al., 2008; Hidaka et al., 2013; Kim and Oh, 2011). The relative low removal of NH_4^+ with silicate addition may still significantly benefit to the stable operation of sludge AD, especially under high organic loading.

In summary, simultaneous in-situ CO_2 sequestration and nutrients removal as well as methane production enhancement could be achieved with silicate addition in AD. The role of silicate was mainly the carrier and supplier of Ca^{2+} and Mg^{2+}. With releasing of equimolar Ca^{2+} and Mg^{2+}, the best performance of nutrients removal coupled with CO_2 sequestration was realized. The increased Ca^{2+} and Mg^{2+} concentration in AD facilitated methane production. Another role of silicate was the pH buffer. The protons generated during VFAs production could be consumed with the silicate for Ca^{2+} and Mg^{2+} release. The increased pH facilitated subsequent precipitation and methane production. Therefore, silicate exerts more benefits than soluble calcium and magnesium salts like $CaCl_2$ and $MgCl_2$. In this study, high purity and well grinded silicate was used. However, for CO_2 and nutrient capture, purity and particle shape of the silicate are not strictly required, silicate slag waste could be adopted to reduce the cost in practical engineering. For large particles of silicate slag waste, a rough grinding should be enough for further application. Though economic analysis was not conducted owing to lack of the accurate price of silicate slag waste, applying silicate slag waste is a potential way to make this approach economic feasibility. For easy retrieving the remained silicate, the added silicate was filled in dialysis bags. In this case, the diffusion of silicate into sludge could be prevented, and the remained silicate could be retrieved by picking up the dialysis bags, while the reaction between silicate and proton, and the release of Ca^{2+} would not be significantly influenced owing to the good ion permeability of dialysis bags. Nonwoven fabric bags can be used instead of dialysis ones during engineering application to reduce the price. The AD performance achieved in this study with silicate addition was attractive, however, studies are required for promoting this approach to practical engineering. The primary concern of this approach is the separation of $MgNH_4PO_4$ and $CaCO_3$, and pipe clogging risk in engineering application. Further studies on fluid mechanics to attenuate precipitate clogging in pipe and processes like centrifugation for precipitate separation are strongly recommended. The innovation of pipe material for less fouling also contributes to the engineering appication of this approach.

4. Conclusion

High CO_3^{2-} concentration could facilitate the formation of MAP under NH_4^+ and PO_4^{3-} concentration simulated to anaerobic digestate. Directed precipitation of Mg^{2+} and Ca^{2+} to MAP and $CaCO_3$ was achieved under Mg^{2+}/Ca^{2+} ratio of 1:1 in simulated anaerobic digestate. Supplementation of 40 g/L magnesium silicate combined with 20 g/L wollastonite in AD decreased CO_2 content from 28.2% to 19.0%, and removed PO_4^{3-} and NH_4^+ by 61.8% and 21.2%, respectively. Methane production was improved by 51.2% with silicate supplementation. This work realized simultaneous in-situ CO_2 sequestration and nutrients removal, as well as methane production enhancement, with silicate mediation, which provides an attractive measure for sludge AD improvement.

Acknowledgements

This study was supported by National Natural Science Foundation of China (No. 51678280, No. 51708253), Special Program for the Taihu Lake Protection of Jiangsu Province (TH2016201), the Fundamental Research Funds for the Central Universities (JUSRP11820), and Postgraduate Research & Practice Innovation Program of Jiangsu Province (SJCX18 0637).

Conflicts of interest

None.

Appendix A. Supplementary data

Supplementary data to this article can be found online at https://doi.org/10.1016/j.biortech.2019.03.004.

References

Abouelenien, F., Kitamura, Y., Nishio, N., Nakashimada, Y., 2009. Dry anaerobic ammonia-methane production from chicken manure. Appl. Microbiol. Biotechnol. 82, 757–764.

Angelidaki, I., Treu, L., Tsapekos, P., Luo, G., Campanaro, S., Wenzel, H., Kougias, P.G.,

2018. Biogas upgrading and utilization: current status and perspectives. Biotechnol. Adv. 36, 452–466.

Azdarpour, A., Asadullah, M., Mohammadian, E., Hamidi, H., Junin, R., Karaei, M.A., 2015. A review on carbon dioxide mineral carbonation through pH-swing process. Chem. Eng. J. 279, 615–630.

Bearat, H., McKelvy, M.J., Chizmeshya, A.V.G., Gormley, D., Nunez, R., Carpenter, R.W., Squires, K., Wolf, G.H., 2006. Carbon sequestration via aqueous olivine mineral carbonation: role of passivating layer formation. Environ. Sci. Technol. 40, 4802–4808.

Cao, X., Harris, W., 2008. Carbonate and magnesium interactive effect on calcium phosphate precipitation. Environ. Sci. Technol. 42, 436–442.

Chen, Y., Cheng, J.J., Creamer, K.S., 2008. Inhibition of anaerobic digestion process: a review. Bioresour. Technol. 99, 4044–4064.

China, S.E.P.A.o., 2002. Standard Methods for the Analysis of Water and Wastewater. China Environmental Science Publishing House, Beijing.

Choi, S., Drese, J.H., Jones, C.W., 2009. Adsorbent materials for carbon dioxide capture from large anthropogenic point sources. ChemSusChem 2, 796–854.

Dang, Y., Zhang, R., Wu, S., Liu, Z., Qiu, B., Fang, Y., Sun, D., 2014. Calcium effect on anaerobic biological treatment of fresh leachate with extreme high calcium concentration. Int. Biodeterior. Biodegrad. 95, 76–83.

Farhang, F., Oliver, T.K., Rayson, M., Bren, G., Stockenhuber, M., Kennedy, E., 2016. Experimental study on the precipitation of magnesite from thermally activated serpentine for CO_2 sequestration. Chem. Eng. J. 303, 439–449.

Fernandez, Y.B., Soares, A., Koch, K., Vale, P., Cartmell, E., 2017. Bioconversion of carbon dioxide in anaerobic digesters for on-site carbon capture and biogas enhancement–a review. Crit. Rev. Environ. Sci. Technol. 47, 1555–1580.

Fonoll, X., Astals, S., Dosta, J., Mata-Alvarez, J., 2015. Anaerobic co-digestion of sewage sludge and fruit wastes: evaluation of the transitory states when the co-substrate is changed. Chem. Eng. J. 262, 1268–1274.

Gu, Y., Li, Y., Li, X., Luo, P., Wang, H., Robinson, Z.P., Wang, X., Wu, J., Li, F., 2017. The feasibility and challenges of energy self-sufficient wastewater treatment plants. Appl. Energy 204, 1463–1475.

Harris, W.G., Wilkie, A.C., Cao, X., Sirengo, R., 2008. Bench-scale recovery of phosphorus from flushed dairy manure wastewater. Bioresour. Technol. 99, 3036–3043.

Hidaka, T., Wang, F., Togari, T., Uchida, T., Suzuki, Y., 2013. Comparative performance of mesophilic and thermophilic anaerobic digestion for high-solid sewage sludge. Bioresour. Technol. 149, 177–183.

Jenicek, P., Bartacek, J., Kutil, J., Zabranska, J., Dohanyos, M., 2012. Potentials and limits of anaerobic digestion of sewage sludge: energy self-sufficient municipal wastewater treatment plant? Water Sci. Technol. 66, 1277–1281.

Kerisit, S., Bylaska, E.J., Felmy, A., 2013. Water and carbon dioxide adsorption at olivine surfaces. Chem. Geol. 359, 81–89.

Kim, D.-H., Oh, S.-E., 2011. Continuous high-solids anaerobic co-digestion of organic solid wastes under mesophilic conditions. Waste Manage. 31, 1943–1948.

Kumar, S., Das, A., Srinivas, G.L.K., Dhar, H., Ojha, V.K., Wong, J., 2016. Effect of calcium chloride on abating inhibition due to volatile fatty acids during the start-up period in anaerobic digestion of municipal solid waste. Environ. Technol. 37, 1501–1509.

Lindeboom, R.E.F., Ferrer, I., Weijma, J., van Lier, J.B., 2013. Silicate minerals for CO_2 scavenging from biogas in Autogenerative High Pressure Digestion. Water Res. 47, 3742–3751.

Linville, J.L., Shen, Y., Schoene, R.P., Nguyen, M., Urgun-Demirtas, M., Snyder, S.W., 2016a. Impact of trace element additives on anaerobic digestion of sewage sludge with in-situ carbon dioxide sequestration. Process Biochem. 51, 1283–1289.

Linville, J.L., Shen, Y., Urgun-Demirtas, M., Snyder, S.W., 2016b. Effect of particle size and doses of olivine addition on carbon dioxide sequestration during anaerobic digestion of sewage sludge at ambient and mesophilic temperatures. Process Biochem. 51, 59–72.

Lombardi, L., Carnevale, E., 2013. Economic evaluations of an innovative biogas upgrading method with CO_2 storage. Energy 62, 88–94.

Montanes, R., Perez, M., Solera, R., 2014. Anaerobic mesophilic co-digestion of sewage sludge and sugar beet pulp lixiviation in batch reactors: effect of pH control. Chem. Eng. J. 255, 492–499.

Praveen, P., Guo, Y.C., Kang, H., Lefebvre, C., Loh, K.C., 2018. Enhancing microalgae cultivation in anaerobic digestate through nitrification. Chem. Eng. J. 354, 905–912.

Salek, S.S., Kleerebezem, R., Jonkers, H.M., Witkamp, G.-J., van Loosdrecht, M.C.M., 2013. Mineral CO2 sequestration by environmental biotechnological processes. Trends Biotechnol. 31, 139–146.

Shahabadi, M.B., Yerushalmi, L., Haghighat, F., 2010. Estimation of greenhouse gas generation in wastewater treatment plants – Model development and application. Chemosphere 78, 1085–1092.

Shahabadi, M.B., Yerushalmi, L., Haghighat, F., 2009. Impact of process design on greenhouse gas (GHG) generation by wastewater treatment plants. Water Res. 43, 2679–2687.

Sun, Q., Li, H., Yan, J., Liu, L., Yu, Z., Yu, X., 2015. Selection of appropriate biogas upgrading technology-a review of biogas cleaning, upgrading and utilisation. Renew. Sustain. Energy Rev. 51, 521–532.

Wang, R.Y., Li, Y.M., Wang, W.H., Chen, Y.G., Vanrolleghem, P.A., 2015. Effect of high orthophosphate concentration on mesophilic anaerobic sludge digestion and its modeling. Chem. Eng. J. 260, 791–800.

Yin, C., Shen, Y., Zhu, N., Huang, Q., Lou, Z., Yuan, H., 2018. Anaerobic digestion of waste activated sludge with incineration bottom ash: enhanced methane production and CO2 sequestration. Appl. Energy 215, 503–511.

Zhang, W., Dai, K., Xia, X.-Y., Wang, H.-J., Chen, Y., Lu, Y.-Z., Zhan, F., Zeng, R.J., 2018a. Free acetic acid as the key factor for the inhibition of hydrogenotrophic methanogenesis in mesophilic mixed culture fermentation. Bioresour. Technol. 264, 17–23.

Zhang, Y., Zhang, L., Liu, H., Gong, L., Jiang, Q., Liu, H., Fu, B., 2018b. Carbon dioxide sequestration and methane production promotion by wollastonite in sludge anaerobic digestion. Bioresour. Technol. 272, 194–201.